

Black Holes and Galaxy Dynamics

David Merritt

Department of Physics and Astronomy, Rutgers University

Abstract. The consequences of nuclear black holes for the structure and dynamics of stellar spheroids are reviewed. Slow growth of a black hole in a pre-existing core produces a power-law cusp, $\rho \sim r^{-\gamma}$, with $\gamma \approx 2$, similar to the steep cusps seen in faint elliptical galaxies. The weaker cusps in bright ellipticals, $\gamma \lesssim 1$, may result from ejection of stars by a coalescing black-hole binary; there is marginal kinematical evidence for such a process having occurred in M87. Stellar orbits in a triaxial nucleus are mostly regular at radii where the gravitational force is dominated by the black hole, $r \lesssim r_g$; however the orbital shapes are not conducive to reinforcing the triaxial figure, hence nuclei are likely to be approximately axisymmetric. In triaxial potentials, a “zone of chaos” extends from a few times r_g out to a radius where the enclosed stellar mass is $\sim 10^2$ times the mass of the black hole; in this chaotic zone, no regular, box-like orbits exist. At larger radii, the phase space in triaxial potentials is complex, consisting of stochastic orbits as well as regular orbits associated with stable resonances. Figure rotation tends to increase the degree of stochasticity. Both test-particle integrations and N -body simulations suggest that a triaxial galaxy responds globally to the presence of a central mass concentration by evolving toward more axisymmetric shapes; the evolution occurs rapidly when the mass of the central object exceeds $\sim 2\%$ of the mass in stars. The lack of significant triaxiality in most early-type galaxies may be a consequence of orbital evolution induced by nuclear black holes.

1. Introduction

The idea that supermassive black holes are generic components of galactic nuclei has come to be widely accepted, due largely to the kinematical detection of dark objects with masses $10^{6-9.5}M_\odot$ at the centers of about a dozen galaxies (Kormendy & Richstone 1995; Jaffe, this volume). The mean mass of these objects – of order $10^{-2.5}$ times the mass of their host spheroids – is consistent with the mass in black holes needed to produce the observed energy density in quasar light given reasonable assumptions about the efficiency of quasar energy production (Chokshi & Turner 1992). The black hole paradigm also explains in a natural way many of the observed properties of energy generation in active galactic nuclei and quasars (Blandford 1990). However it has long been clear that supermassive black holes might be important from a purely stellar-dynamical point of view: both within the nucleus, where the gravitational force

is dominated by the black hole; but also at much larger radii, if a substantial number of stars are on orbits that carry them into the center (Gerhard & Binney 1985). Recent work, reviewed here, has developed these ideas and given support to the view that supermassive black holes may be important for understanding many of the systematic, large-scale properties of elliptical galaxies and bulges.

2. Nuclear Dynamics

2.1. Cusp formation

The luminosity densities of early-type galaxies and bulges are well approximated as power-laws, $\nu \propto r^{-\gamma}$, inside of a “break radius” r_b (Crane et al. 1993; Gebhardt et al. 1996). The break radius is difficult to measure in fainter galaxies whose steep cusps have roughly the same power-law index ($\gamma \approx 2$) as the larger-radius profile. In bright galaxies, $M_v \lesssim -20$, the central cusps are shallower ($\gamma \lesssim 1$) and the luminosity profiles show a definite change in slope at $r \approx r_b$ (Kormendy, this volume). In these galaxies, r_b scales roughly with total luminosity (Faber et al. 1997); spheroids with $M_v \approx -21$ have $r_b \approx 50$ pc, easily resolvable from the ground for nearby galaxies.

To what extent are the stellar cusps attributable to the presence of a black hole? The gravitational force from a black hole of mass M_h would dominate the force from the stars within a radius r_g such that $M_*(< r_g) = M_h$. This radius is roughly comparable to r_b in the handful of galaxies for which both r_b and M_h can be accurately measured; for instance, in M87, where M_h is well constrained by the kinematics of a gas disk (Macchetto et al. 1997), $r_g \approx r_b \approx 300$ pc. However the black hole can strongly influence the motions of stars only inside the (typically smaller) radius $r_h = GM_h/\sigma_*^2$, the “radius of influence,” where orbital velocities around the black hole are comparable to stellar velocity dispersions. M87 has $r_h \approx 60$ pc, much smaller than r_g or r_b and barely resolvable from the ground.

One expects to observe photometric and kinematic features in the stellar distribution near r_h ; indeed, the upturn in stellar velocities that occurs near this radius is one signature of a black hole. However few if any galaxies exhibit a clear feature in the stellar luminosity profile inside of r_b (Gebhardt et al. 1996), a fact that must be explained by any model of cusp formation.

One widely-discussed model for the formation of stellar cusps is the slow growth of a black hole in a pre-existing, constant-density core. “Slow” here means on a time scale long compared to stellar orbital periods, $\sim 10^{6-7}$ yr, thus guaranteeing conservation of orbital actions; the assumption is a reasonable one if black holes grew on the Salpeter time scale, $t_s \approx 10^{7-8}$ yr (Krolik 1999). If the core was initially isothermal, and if the final mass of the black hole is less than the initial core mass, the final density satisfies $\rho \propto r^{-\gamma}$, $\gamma = 1.5$, for $r \lesssim r_h$ (Peebles 1972; Young 1980). An interesting feature of the Peebles-Young model is the smooth, nearly inflectionless form of the final density profile between r_h and r_c , the initial core radius. Van der Marel (1999; this volume) took advantage of this fact, associating r_c with the observed break radius r_b . He was able to fit the weak power-law cusps of bright ellipticals to the region $r_h \lesssim r \lesssim r_c$ where the Peebles-Young profile is locally well approximated by a shallow power law. The steep cusps of faint ellipticals were less accurately reproduced.

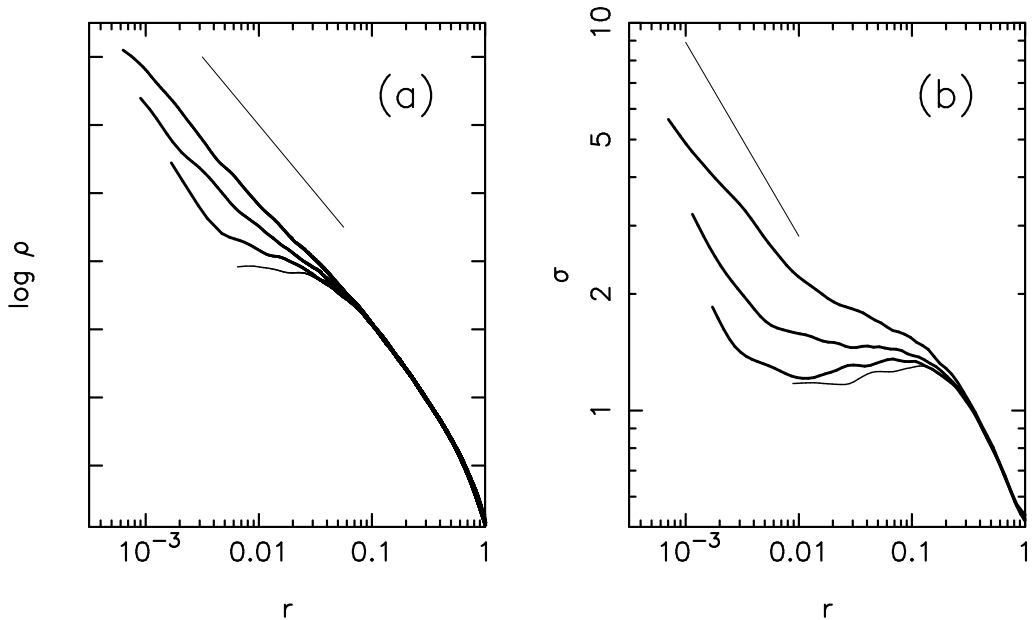


Figure 1. Cusp formation by adiabatic growth of a black hole (Merritt & Quinlan 1998). The initial model (thin curves) is a triaxial ellipsoid, shown here spherically symmetrized; heavy curves are the final models after growth of a central point containing 0.3%, 1% and 3% of the stellar mass. **(a)** Stellar density profiles $\rho(r)$; the thin line has a logarithmic slope of -2 . These cusps are steeper than the $\rho \propto r^{-1.5}$ cusps that form in initially isothermal cores. **(b)** Velocity dispersion profiles $\sigma(r)$. The small-radius dependence is $\sigma \sim r^{-1/2}$ (thin line).

The initial conditions adopted by Peebles, Young and van der Marel – isothermal spheres with large core radii – are computationally convenient but not very compelling from a physical point of view. Formation of galaxies through hierarchical clustering (e. g. Primack et al., this volume) or collapse (e.g. May & van Albada 1984) tends to make systems with small or nonexistent cores and with phase space densities that rise more rapidly than $\sim e^{-aE}$ near the center. Growing a black hole in such a galaxy produces a steeper cusp than in an initially isothermal core, typically with $\gamma \gtrsim 2$ (Quinlan et al. 1995; Merritt & Quinlan 1998; Fig. 1). This is just the slope characteristic of the central regions of faint ellipticals and it would seem reasonable to attribute the cusps in these galaxies to black holes. The absence of a prominent break radius in faint ellipticals would imply that the initial core mass (if there was a core) did not greatly exceed the final mass of the black hole.

Dissipation is often invoked as a possible mechanism for making steep cusps (e.g. Faber et al. 1997) though simulations of dissipative core formation (e.g. Mihos & Hernquist 1994) have so far failed to produce power-law profiles.

The weak cusps in brighter ellipticals are not so naturally explained via the adiabatic growth model: not only are they much shallower than $\rho \sim r^{-2}$ but – as Fig. 1 shows – the transition from $\rho \sim r^{-2}$ at $r \lesssim r_h$ to $\rho \sim \text{constant}$ at $r \sim r_c$ leaves an inflection in the density profile if $r_h < r_c$, and such inflections are rarely if ever seen. A more natural formation model for weak cusps would predict only

one characteristic radius, r_b . Such a model was proposed by Ebisuzaki, Makino and Okumura (1991). These authors noted that the coalescence of two black holes following a galaxy merger would transfer energy from the binary to the stars in the nucleus, creating a low-density core with mass comparable to the combined mass of the two black holes. In their model (further developed in Makino & Ebisuzaki 1996 and Makino 1997), the break radius r_b measures the size of the region “scoured out” by the binary black hole – consistent with the observed, rough equality of r_b and r_g . The predicted density profile within r_b is tolerably close to a power law with index $\gamma \lesssim 1$; in this model, the observed trend of decreasing γ with increasing luminosity would simply reflect a greater role for mergers in the formation of brighter galaxies.

One way to discriminate between the adiabatic growth and binary black hole models for cusp formation is via their very different predictions about the stellar kinematics near the black hole. Slow growth of a black hole leaves the shape of the stellar velocity ellipsoid nearly unchanged (Young 1980; Goodman & Binney 1984), even at radii where σ_* increases substantially; the reason is that orbital eccentricities are almost unaffected by adiabatic changes in the potential (Lynden-Bell 1963). By contrast, ejection of stars by a coalescing black hole binary produces a core with strongly circularly-biased motions, since stars on radial trajectories are more likely to interact with the binary (Quinlan 1996). Quinlan & Hernquist (1997) and Nakano & Makino (1999) found that the velocity anisotropy $\beta \equiv 1 - \sigma_t^2/\sigma_r^2$ in an initially isotropic core can drop as low as ~ -1 after the ejection of stars is complete.

Stellar velocity anisotropies are difficult to extract from integrated spectra; the task becomes much easier if the form of the gravitational potential is known a priori, since the anisotropy then follows directly from the line-of-sight velocity dispersion profile (Binney & Mamon 1982). The velocity polarization predicted by the binary black hole model is therefore best looked for in a galaxy where M_h has been determined independently from the stellar data. M87 is such a galaxy, and in fact the ground-based stellar data, combined with the Macchetto et al. (1997) estimate of M_h , imply a substantial anisotropy, $\beta \approx -1$, at $r \lesssim r_h$ (Merritt & Oh 1997). However the statistical significance of the result is small due to the low central surface brightness of this galaxy. Planned observations of M87 and other galaxies with STIS on HST should soon resolve this issue.

2.2. Nonspherical nuclei

The gravitational potential in the vicinity of the black hole, at $r \lesssim r_g$, is nearly Keplerian; forces from the stars in the cusp constitute a small perturbation, causing orbits to precess. In an axisymmetric galaxy, this precession converts an otherwise closed, elliptical orbit into a tube orbit which fills a doughnut-shaped region around the symmetry axis. Tube orbits avoid the center due to conservation of angular momentum; hence a star on a tube orbit can come only so close to the black hole. The situation is very different, and much more interesting, in non-axisymmetric or triaxial nuclei. While tube orbits still exist in such potentials, orbits that pass arbitrarily close to the center are possible as well.

Figure 2 illustrates how the character of “box-like” orbits – orbits with stationary points and (in an integrable potential) filled centers – varies with

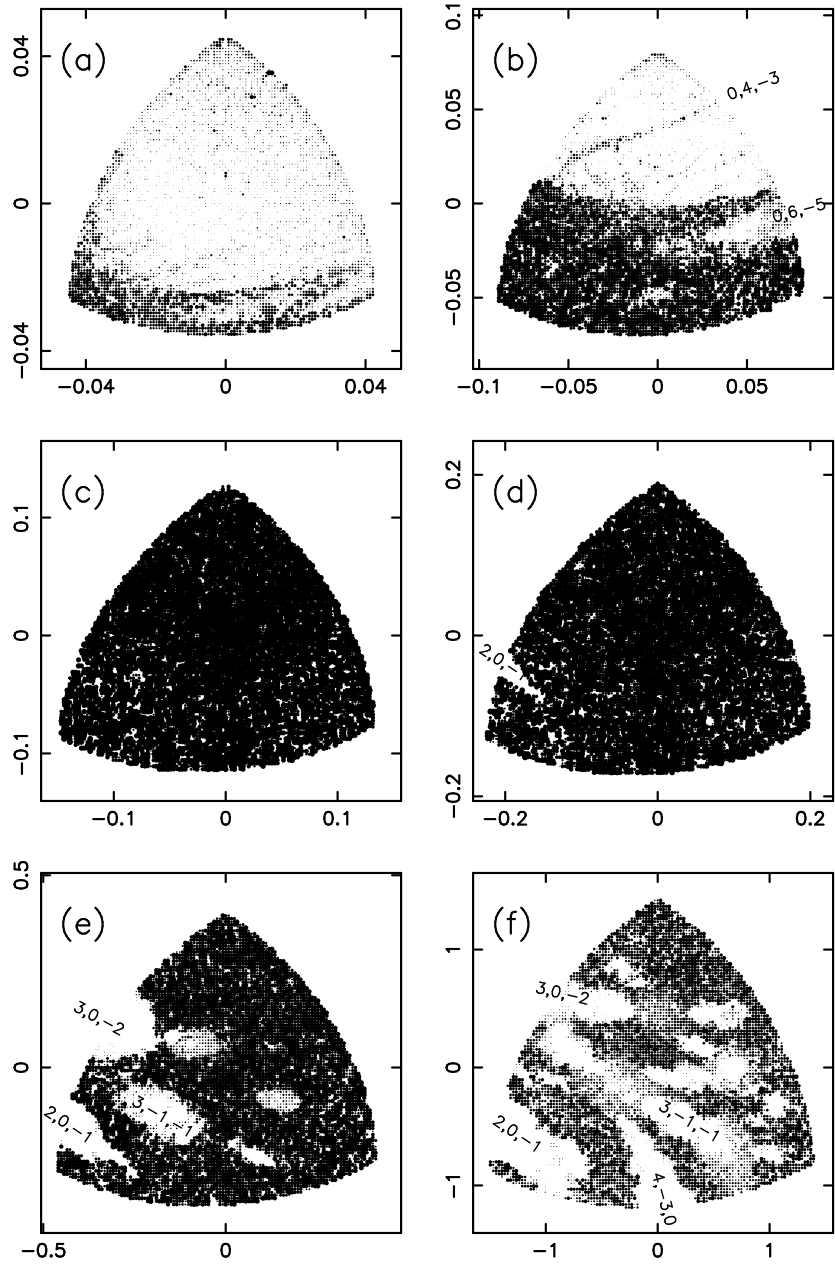


Figure 2. Properties of box-like orbits in a triaxial potential containing a central point mass. Each panel shows one octant of an equipotential surface; the z (short) axis is vertical and the x (long) axis is to the left. Orbits were started on this surface with zero velocity. The degree of stochasticity is indicated by the grey scale; white regions correspond to regular orbits. Resonance zones are labelled by their defining integers. The ratio M_h/M_* of black hole mass to enclosed stellar mass is (a) 0.33, (b) 0.22, (c) 0.13, (d) 0.088, (e) 0.032 and (f) 0.0079. The half-mass radius of the model is approximately one. Near the black hole (a), orbits are mostly regular; in the “zone of chaos” (c, d), almost all box-like orbits are chaotic; and at large radii (f), regular and stochastic orbits co-exist.

distance from the central black hole in a triaxial potential. Near the black hole, $r \lesssim r_g$, almost all box-like orbits are regular, i.e. non-chaotic, respecting three isolating integrals of the motion. Such orbits in the planar geometry have been dubbed “lenses” by Sridhar & Touma (1999); in three dimensions, the orbits are shaped like pyramids with rectangular bases. The black hole lies just inside the vertex of the pyramid, at the focus of the precessing ellipse, and the pyramid’s central axis is coincident with the short (z) axis of the triaxial figure. A superposition of two such orbits, oriented above and below the $x - y$ plane, is symmetric and looks very much like the regular box orbits in integrable triaxial potentials (de Zeeuw 1985). However the latter are aligned with the *long* axis of the triaxial figure, making them much more useful for self-consistently reconstructing the stellar density.

At larger radii, $r \gtrsim r_g$, the potential is no longer approximately Keplerian and the integrability is lost – box-like orbits are generically stochastic (Fig. 2c, d). This “zone of chaos” in triaxial potentials extends from a few times r_g outward to much larger radii, as discussed below.

Could the predominantly regular orbits – pyramids and tubes – within $\sim r_g$ be used to self-consistently reconstruct a triaxial nucleus containing a central black hole? The question is in principle straightforward to answer though as yet no attempts have been made. Two studies (Kuijken 1993; Syer & Zhao 1998) addressed the self-consistency problem for scale-free, non-axisymmetric disks with divergent central densities. The major families of box-like orbits in both of these planar potentials are 2 : 1 “bananas”; in spite of having a favorable orientation parallel to the long axis, the banana orbits were found to be too limited in their range of shapes to reproduce the assumed figure. Pyramid orbits have even less favorable shapes and it is reasonable to expect the triaxial self-consistency problem for black hole nuclei to be at least as narrowly constrained as that for scale-free disks.

It therefore seems likely that significant triaxiality would be difficult to maintain near the center of a galaxy containing a supermassive black hole: both at radii $r \lesssim r_g$, because of the unfavorable orientation of the (predominantly regular) orbits; and at radii $r \gtrsim r_g$, because of chaos.

In advance of more definite theoretical predictions, a number of workers have recently investigated the isophotal shapes of early-type galaxies at radii near r_b . Quillen (this volume) finds a change in ellipticity and boxiness between $\sim r_b$ and a few times r_b in the isophotes of two galaxies; the change is in the direction of more elongated and boxier isophotes at large radii. Tymann (cited in Bender, this volume) also finds less boxy isophotes inward of r_b in a sample of early-type galaxies. Ryden (1998; this volume) shows that bright ellipticals as a class exhibit rounder isophotes at radii of a few times r_b than at larger radii; the effect is consistent with more nearly axisymmetric shapes at smaller radii, since oblate spheroids are more likely than triaxial ellipsoids to appear round under random projection.

These results suggest a possible change in the shapes or orbital compositions of galaxies near r_b , perhaps in the direction of more axisymmetric configurations at smaller radii. As Quillen and Ryden both note, such changes could reflect the constraints that a black hole imposes on the shapes of orbits, or they could be relics of the core formation process, or both. Distinguishing between these

possibilities will be easier once the self-consistency problem for black-hole nuclei is better understood.

Orbits like the pyramids are not centered on the black hole, a consequence of the near-Keplerian nature of the potential. Sridhar & Touma (1999) noted that off-center orbits can persist even in nuclei where the black hole itself is offset from the center of the stellar spheroid; furthermore they identified one orbit family for which the orbital offset was in the same direction as that of the spheroid. One could imagine using such orbits to construct self-consistent, lopsided nuclei along the lines of the conceptual model proposed by Tremaine for M31 (1995). One attempt, using an N -body code, is described by Jacobs & Sellwood (this volume); these authors were unable to construct long-lived lopsided disks unless the disk mass was less than a few percent of the mass of the black hole, substantially smaller than the estimated mass of the stellar disk in M31 (Kormendy & Bender 1999).

3. Large-Scale Dynamics

3.1. Regular and stochastic orbits

The gravitational influence of a nuclear black hole can extend far beyond r_g in a non-axisymmetric galaxy, since orbital angular momenta are not conserved and stars with arbitrarily large energies can pass close to the center (Gerhard & Binney 1985). In a triaxial potential containing a central point mass, the phase space divides naturally into three regions depending on distance from the center (Fig. 2). In the innermost region, $r \lesssim r_g$, the potential is dominated by the black hole and the motion is essentially regular, as discussed above. At intermediate radii (Fig. 2c, d), the black hole acts as a scattering center, rendering almost all of the center-filling orbits stochastic. This “zone of chaos” extends outward from a few times r_g to a radius where the enclosed stellar mass is roughly 10^2 times the mass of the black hole. If M_h exceeds $\sim 10^{-2} M_{sph}$, as it appears to do in a few galaxies, the “zone of chaos” includes essentially the entire potential outside of $\sim r_g$. However if $M_h \lesssim 10^{-2} M_{sph}$, there is a third, outer region in which the phase space is a complex mixture of chaotic and regular trajectories (Fig. 2e, f). In the absence of a central point mass, the orbital structure of a triaxial potential resembles this complex outer region at all energies (Schwarzschild 1993; Merritt & Fridman 1996; Carpintero & Aguilar 1998; Papaphillipou & Laskar 1998; Valluri & Merritt 1998; Wachlin & Ferraz-Mello 1998).

The complexity of the phase space far from the black hole is a consequence of resonances. A resonant orbit is one for which the fundamental frequencies $\omega_i, i = 1, 2, 3$ on the invariant torus are “commensurate,” satisfying a relation of the form $m_1\omega_1 + m_2\omega_2 + m_3\omega_3 = 0$ with integer m_i . In the case of 2D motion, a resonant orbit is closed, returning to its starting point after a time $T = 2\pi|m_2|/\omega_1 = 2\pi|m_1|/\omega_2$. In three dimensions, resonances do not imply closure; instead, a resonant trajectory is confined for all time to a two-dimensional sub-manifold of its 3-torus (Valluri & Merritt, this volume). Such an orbit is thin, densely filling a membrane in configuration space.

Resonant tori play roughly the same role, in three dimensions, that closed orbits play in two, generating families of regular orbits when stable and stochas-

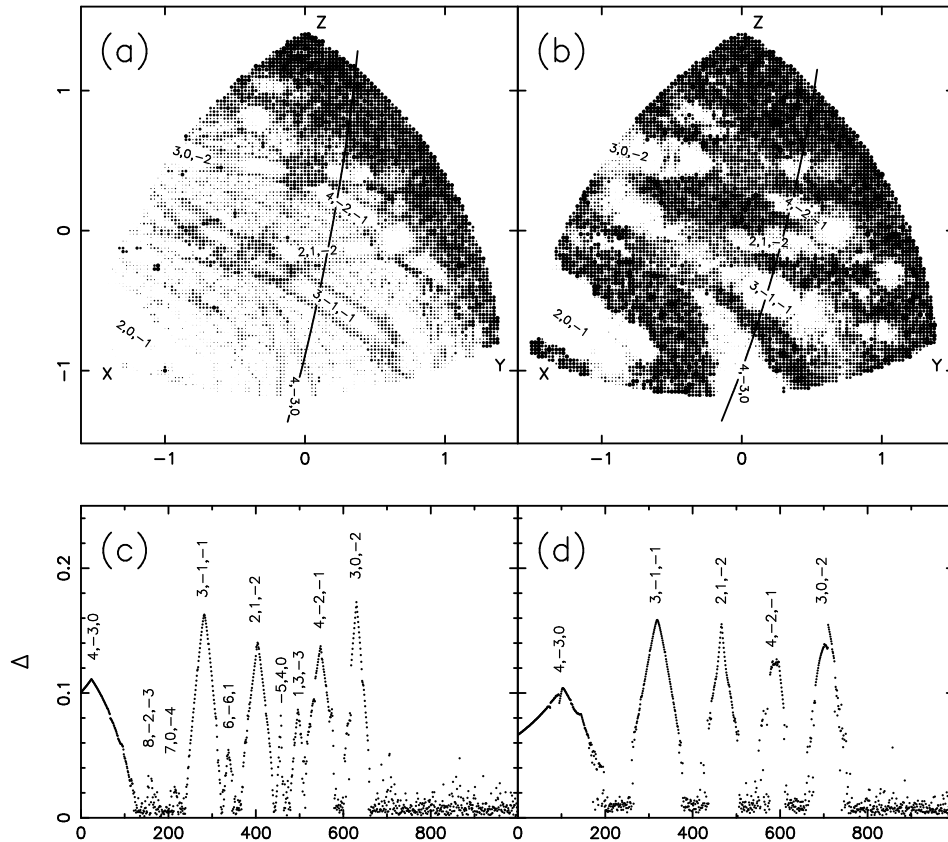


Figure 3. Resonances in triaxial potentials (Merritt & Valluri 1999). The mass model in (a) has a weak ($\gamma = 0.5$) cusp and no black hole; in (b) the black hole contains 0.3% of the total mass. Both equipotential surfaces lie close to the half-mass radius. The grey scale measures the degree of stochasticity of orbits started with zero velocity on the equipotential surface, as in Fig. 2. Stable resonance zones – the white bands in (a) and (b) – are labelled by the order (m_1, m_2, m_3) of the resonance. Panels (c) and (d) show the pericenter distance Δ of a set of 10^3 orbits with starting points along the heavy solid lines in (a) and (b).

tic orbits when unstable (Merritt & Valluri 1999). In triaxial potentials, the main source of instability is gravitational deflections from the central point mass; stable orbits are ones that avoid the center. Tube orbits achieve this via a 1 : 1 resonance in one of the principal planes; box orbits are generically center-filling, but a box orbit associated with a sufficiently low-order resonance can also avoid the center by a wide enough margin to remain stable.

The degree to which this is possible depends on the steepness of the central force gradient (Valluri & Merritt 1998). When the central singularity is weak – for instance, a $\rho \propto r^{-\gamma}$ stellar cusp – box-like orbits can remain stable even when their pericenter distances are small. Phase space then consists of a large number of intersecting and overlapping resonance zones, some of high order, corresponding to thin orbits with many sheets (Fig. 3a). When the central singularity is stronger – e.g. a central point mass – only a handful of low-order

resonances can maintain sufficient pericenter distance to remain stable (Fig. 3b); high-order resonances typically generate stochastic zones. As the mass of the central point is increased, fewer and fewer of the resonant orbits are able to avoid the center by a wide enough margin and the phase space undergoes a transition to global stochasticity – essentially all of the box-like trajectories are chaotic. While this transition has only been studied in a handful of model potentials, it seems to occur whenever the black hole mass exceeds $\sim 2 - 3\%$ of the enclosed mass in stars (Merritt & Quinlan 1998; Valluri & Merritt 1998; Merritt & Valluri 1999).

The influence of figure rotation on the orbital composition of triaxial potentials has not yet been systematically studied. Valluri (this volume) finds that figure rotation tends to increase the degree of orbital stochasticity, apparently because the Coriolis forces broaden orbits that would otherwise be thin, driving them into the destabilizing center.

3.2. Black-hole-induced evolution

Stochastic motion introduces a new time scale into galactic dynamics, the mixing time (Kandrup & Mahon 1994; Kandrup, this volume). Mixing is the process by which a non-uniform distribution of particles in phase space relaxes to a uniform distribution, at least in a coarse-grained sense. A weak sort of mixing, called phase mixing, occurs even in integrable potentials, as particles on adjacent tori gradually move apart (Lynden-Bell 1967); phase mixing is responsible for the fact that the coarse-grained phase space density in relaxed systems is nearly constant around tori. Mixing in chaotic systems can be much more effective than phase mixing, since stochastic trajectories are exponentially unstable and not confined to tori. Chaotic mixing is also irreversible in the sense that an infinitely fine tuning of velocities would be required in order to undo its effects.

Mixing driven by a central black hole converts all of the stochastic trajectories at a single energy into an invariant ensemble whose shape is similar to that of an equipotential surface, hence rounder than the figure. Two consequences are likely: the galaxy should become rounder, or at least more axisymmetric, due to the loss of the regular orbits needed to maintain triaxiality; and sharp features in the phase-space distribution should be smoothed out. Mixing induced by a central singularity ceases if the stellar distribution reaches an axisymmetric state since few stars are then able to approach the destabilizing center.

The rate at which mixing would induce such changes can be estimated by integrating trajectories in fixed triaxial potentials. Such experiments (Kandrup & Mahon 1994; Mahon et al. 1995; Merritt & Valluri 1996; Valluri & Merritt 1998) reveal a strong dependence of the mixing rate on the structure of phase space. In regions containing both regular and stochastic trajectories – e.g. the two outermost shells of Figure 2 – mixing is inefficient, presumably because the invariant tori of the regular orbits hinder the diffusion of the stochastic orbits. In regions where the motion is almost fully chaotic – e.g. the “zone of chaos” in Figure 2 – mixing occurs very rapidly, in a few crossing times. Orbits in such regions lose all memory of their initial conditions after just a few oscillations.

Norman, May & van Albada (1985) made one of the first attempts to simulate the large-scale response of a galaxy to the orbital evolution induced by a central black hole. These authors observed only a slight response at the centers

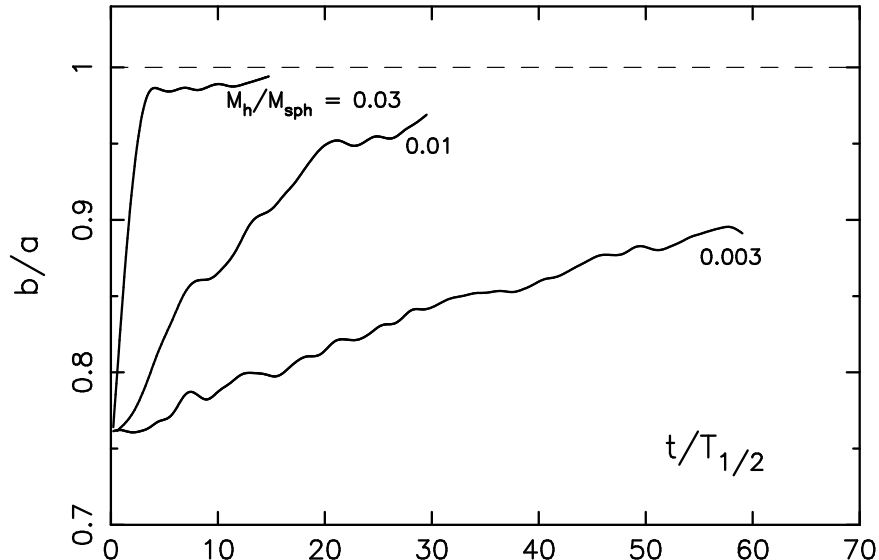


Figure 4. Response of an initially triaxial galaxy to growth of a central point mass (adapted from Merritt & Quinlan 1998). The intermediate-to-long axis ratio b/a , defined by the most-bound 50% of the stars, is plotted as a function of time; $T_{1/2}$ is the period of a circular orbit at the half-mass radius in a spherical model with the same radial distribution of mass. The growth time of the central mass was $\sim 5T_{1/2}$ for the two smaller values of M_h and $\sim 2T_{1/2}$ for the larger value.

of their N -body models; however their initial conditions were almost precisely axisymmetric, thus guaranteeing that the influence of the black hole would be limited to $r \lesssim r_g$. More dramatic evolution was seen in a number of subsequent studies of dissipative galaxy formation (e.g. Katz & Gunn 1991; Udry 1993; Dubinski 1994). These authors used N -body codes to simulate the accumulation of mass at the centers of initially triaxial galaxies or halos; in each case, evolution toward more axisymmetric shapes was observed when the central mass exceeded a few percent of the mass in stars. Barnes (1996; this volume) observed a similar response in N -body simulations of mergers between disk galaxies: purely stellar-dynamical mergers produced strongly triaxial remnants, but adding as little as 1% of the mass in the form of a dissipative component resulted in nearly axisymmetric final shapes. The evolution toward axisymmetry seen in these simulations is sometimes loosely attributed to “dissipation,” but in fact it is purely a stellar dynamical effect: the stars respond to the “gas” only insofar as the latter affects the gravitational potential.

Merritt & Quinlan (1998) repeated the Norman et al. (1985) experiments, using initial models that were significantly triaxial at all radii. They observed a global response toward axisymmetry as the mass of the central point was increased; the rate of evolution was found to depend strongly on the ratio of black hole mass to galaxy mass (Fig. 4). When M_h/M_{sph} was 0.3%, the galaxy evolved in shape over $\sim 10^2$ orbital periods, whereas increasing M_h/M_{sph} to 3% caused the galaxy to become almost precisely axisymmetric in little more

than a crossing time. Rapid evolution toward axisymmetry occurred at any radius whenever the “black hole” mass exceeded ~ 0.025 times the enclosed stellar mass – roughly the same mass ratio at which the regular box-like orbits disappear (Fig. 2).

These experiments provide a natural explanation for the absence of significant triaxiality in most elliptical galaxies (Franx, de Zeeuw & Illingworth 1991). Based on Fig. 4, a galaxy with a “typical” black hole, $M_h/M_{sph} \approx 0.003$, would evolve to axisymmetry in roughly 100 periods of the half-mass circular orbit; this time span is of order a galaxy lifetime for elliptical galaxies with $M_v \approx -19$ or -20 . Fainter ellipticals have generally shorter crossing times and hence should be weakly triaxial at best; brighter ellipticals might still retain their (merger-induced?) triaxial shapes. These predictions are consistent with what little is known about the statistics of elliptical galaxy intrinsic shapes (Ryden 1996; Tremblay & Merritt 1996; Bak & Statler 1999).

Orbital evolution induced by a black hole should smooth out the stellar phase-space distribution at the same time that it destroys triaxiality. In fact Merritt & Quinlan (1998) noted a striking change in the isophotal shapes of their N -body models, from strongly peanut-shaped at the start to nearly elliptical after the black hole was in place. Boxy or peanut-shaped isophotes are a natural consequence of a non-smooth phase space density (Binney & Petrou 1982). One might therefore predict a correlation between triaxiality and boxiness in real galaxies, since the orbital evolution induced by a nuclear black hole would tend to eliminate the two in tandem. Kormendy & Bender (1996) noted just such a correlation; furthermore the majority of boxy ellipticals are bright (Bender, this volume), consistent with the expected, longer time scales for orbital evolution in brighter galaxies.

It is remarkable that the minimum black hole mass required to induce rapid evolution in the orbital composition of a triaxial ellipsoid – $M_h/M_{sph} \approx 2\%$ – is essentially equal to the maximum value of M_h/M_{sph} observed in real galaxies (Kormendy et al. 1996; Cretton & van den Bosch 1999). This agreement could be fortuitous, or it could point to a connection between the fueling of black holes and the shapes of their host spheroids.

References

- Bak, J. & Statler, T. S. 1999, “The Intrinsic Shape Distribution of a Sample of Elliptical Galaxies” (preprint)
- Barnes, J. E. 1996, in *The Formation of Galaxies*, Proceedings of the V Canary Islands Winter School of Astrophysics, ed. C. Muñoz-Tuñón (Cambridge: Cambridge University Press), 399
- Binney, J. J. & Mamon, G. A. 1982, *MNRAS*, 200, 361
- Binney, J. & Petrou, M. 1985, *MNRAS*, 214, 449
- Blandford, R. D. 1990, in *Active Galactic Nuclei, Saas-Fee Advanced Course 20*, eds. T. J.-L. Courvoisier & M. Mayor (Springer, Berlin), 161
- Carpintero, D. D. & Aguilar, L. A. 1998, *MNRAS*, 298, 1
- Chokshi, A. & Turner, E. L. 1992, *MNRAS*, 259, 421
- Crane, P. et al. 1993, *AJ*, 106, 1371
- Cretton, N. & van den Bosch, F. C. 1999, *ApJ*, 514, 704
- de Zeeuw, P. T. 1985, *MNRAS*, 216, 273

Dubinski, J. 1994, ApJ, 431, 617
 Ebisuzaki, T., Makino, J. & Okumura, S. K. 1991, Nature, 354, 212
 Faber, S. M. et al. 1997, AJ, 114, 1771
 Franx, M., Illingworth, G. & de Zeeuw, T. 1991, ApJ, 383, 112
 Gebhardt, K. et al. 1996, AJ, 112, 105
 Gerhard, O. & Binney, J. 1985, MNRAS, 216, 467
 Goodman, J. & Binney, J. 1984, MNRAS, 207, 511
 Kandrup, H. E. & Mahon, M. E. 1994, Phys. Rev. E, 49, 3735
 Katz, N. & Gunn, J. E. 1991, ApJ, 377, 365
 Kormendy, J. & Bender, R. 1996, ApJ, 464, L119
 Kormendy, J. & Bender, R. 1999, "The Double Nucleus and Central Black Hole of M31"
 (preprint)
 Kormendy, J. & Richstone, D. O. 1995, ARA&A, 33, 581
 Kormendy, J. et al. 1996, ApJ, 459, L57
 Krolik, J. H. 1999, Active Galactic Nuclei (Princeton: Princeton University Press), 127
 Kuijken, K. 1993, ApJ, 409, 68
 Lynden-Bell, D. 1963, The Observatory, 932, 23
 Lynden-Bell, D. 1967, MNRAS, 136, 101
 Macchetto, F. et al. 1997, ApJ, 489, 579
 Mahon, M. E., Abernathy, R. A., Bradley, B. O. & Kandrup, H. E. 1995, MNRAS, 275, 443
 Makino, J. 1997, ApJ, 478, 58
 Makino, J. & Ebisuzaki, T. 1996, ApJ, 465, 527
 May, A. & van Albada, T. S. 1984, MNRAS, 209, 15
 Merritt, D. & Fridman, T. 1996, ApJ, 460, 136
 Merritt, D. & Oh, S. P. 1997, AJ, 113, 1279
 Merritt, D. & Quinlan, G. D. 1998, ApJ, 498, 625
 Merritt, D. & Valluri, M. 1996, ApJ, 471, 82
 Merritt, D. & Valluri, M. 1999, AJ, 118
 Mihos, M. J. & Herquist, L. 1994, ApJ, 437, L47
 Nakano, T. & Makino, J. 1999, ApJ, 510, 155
 Norman, C., May, A. & van Albada, T. 1985, ApJ, 296, 20
 Papaphilippou, Y. & Laskar, J. 1998, A&A, 329, 451
 Peebles, P. J. E. 1972, Gen. Rel. Grav., 3, 63
 Quinlan, G. D. 1996, NewA, 1, 35
 Quinlan, G. D. & Hernquist, L. 1997, NewA, 2, 533
 Quinlan, G. D., Hernquist, L. & Sigurdsson, S. 1995, ApJ, 440, 554
 Ryden, B. S. 1996, ApJ, 461, 146
 Ryden, B. S. 1998, astro-ph/9811058
 Schwarzschild, M. 1993, ApJ, 409, 563
 Sridhar, S. & Touma, J. 1999, MNRAS, 303, 483
 Syer, D. & Zhao, H.-S. 1998, MNRAS, 296, 407
 Tremaine, S. 1995, AJ, 110, 628
 Tremblay, B. & Merritt, D. 1996, AJ, 111, 2243
 Udry, S. 1993, A&A, 268, 35
 Valluri, M. & Merritt, D. 1998, ApJ, 506, 686
 van der Marel, R. 1999, AJ, 117, 744
 Wachlin, F. C. & Ferraz-Mello, S. 1998, MNRAS, 298, 22
 Young, P. J. 1980, ApJ, 242, 1232